VOL. 12, NO. 5, MARCH 2017 ISSN 1819-6608
ARPN Journal of Engineering and Applied Sciences

www.arpnjournals.com

MODELING AND ESTIMATE OF THE STRAIN-STRESS STATE OF A BUS BODY PILLAR WITH ACCOUNT FOR GEOMETRICAL NONLINEARITY

N. A. Ovchinnikov, V. I. Zhigulsky, E. A. Kozyreva and O. V. Chefranova
Don State Technical University, Shakhty, Rostov Region, Russia
E-Mail: NikolaOv@yandex.ru

ABSTRACT

The paper considers practical problem solving in passive bus safety and particularly modeling of the strain-stress state of bus body elements under the safety and structural strength conditions. The authors of the paper present the results of the pursuance of numerical research in supporting capacity of the side window bus body pillars. The paper evaluates the detailed finite element model of a bus body pillar with account for geometrical nonlinearity. The realization of finite element analysis of the strain-stress state of a bus body pillar is presented for simple and compound bending. Modeling was made by using the opportunities of ANSYS packaged programs.

Keywords: bus, body, body pillar, passive safety, strength, geometrical nonlinearity, physical nonlinearity, body deflection, crushing load, safe operation life, residual operation life.

BASES OF ACCOUNTING ESTIMATE OF STRUCTURES ACCOUNTING FOR CONDITIONS AND ASSUMPTIONS

Accounting estimate of body structures means the consideration of their component behavior in emergencies influenced by arising elasto-plastic and large plastic strains [1].

The sequence of the evaluation of any accounting estimate by the finite-element method is standard [12]. This paper presents some approaches to accounting estimate of the strength properties of the bus body elements by the finite-element method [13].

The evaluation by the finite-element method demands any structure (geometrical model) being a finite number of elementary volumes. All elements have a simple form and the simplified strain-stress state.

Mechanical behavior of elements, as well as the whole structure, can be described from the three perspectives. These perspectives are based on estimate of physical behavior of strained bearing structure components and are presented as follows:

- imposed and internal forces should be in balance [2];
- adjacent elements after deformation should not vary from each other and interpenetrate, and the boundary nodes of the considered parts should follow the boundary conditions [3];
- connection between tension and strains is determined by physical relation of the theory of elasticity and plasticity [4, 12].

The structure evaluation presents two types of nonlinearity [12]. The first one is physical nonlinearity connected with nonlinearity of the dependency $\sigma = f(\varepsilon)$ that characterizes the structure material in the elasto-plastic part. The second one is geometrical nonlinearity that takes place when the structure displacement causes significant changes of its configuration. The consideration of these types of nonlinearity leads to the resolving set of equations containing nonlinear terms of fractional definable main unknown values.

When estimating of body structures [5, 6] both static nonlinear and dynamic problem solving is possible. Static problems are solved if estimation of supporting capacity of the body structure in the conditions of static loading is necessary [7, 8]. Dynamic problems are solved in theoretical estimating of safety and supporting capacity of structures influenced by shock stress [9, 10].

The present research offers static problem solving in nonlinear putting with account for geometrical nonlinearity by using the ANSYS packaged programs [11].

LINEAR STABILITY ANALYSIS BY THE FINITE-ELEMENT METHOD

The equation of balance of the finite-element model in matrix form is as follows [12]:

$$[\,[K] + \lambda\,[K_r]\,]\,\{W\} = 0,$$

where $[K]$ and $[K_r]$ - are global matrixes of total and geometrical stiffness;

λ - is a loading parameter (scalar quantity);

$\{W\}$ - is a vector of nodal displacement of an assemblage of elements.

After the loss of stability nodal displacement becomes uncertain. A mathematical criterion of the loss of stability is the determinant equal to zero:

$$det\,[\,[K] + \lambda\,[K_r]\,] = 0$$

Thus, the determinant excludes the “excess” lines and columns, rising to node numbers to which constraints are imposed. Thus, the order of a resulting set of equations is always lower than the order of a global stiffness matrix. From the computational viewpoint, the determination of

the parameter λ by the disclosure of a determinant of the high order and the solution of the corresponding transcendental equation is unreal. Therefore, analysis of the finite-element model stability as the generalized problem of its values, allowing the direct solution of the following equation will be conducted [12]:

$$[K]\{X\} = -\lambda_{min}[K_г]\{X\}, \quad (1)$$

where λ_{min} - is an unknown smallest eigen value;
$\{X\}$ - is an eigenvector vector, characterizing a possible form of the loss of stability.

In this formulation the value λ_{min} that makes a geometrical stiffness matrix compensate the total stiffness matrix influence should be determined. From the physical viewpoint, the value λ_{min} is the critical load $P_{кр}$, corresponding to the loss of stability.

The solution of this mixed set of algebraic equations demands the two special iterative algorithms.
The first algorithm is based on the Rayleigh quotient [12]:

$$\lambda_{min}^{(k+1)} = \frac{\{X\}_{k+1}^T [K]\{X\}_{k+1}}{\{X\}_{k+1}^T [K_г]\{X\}_{k+1}}$$

The process of successive approximations is stopped when

$$\frac{\left|\lambda_{min}^{(k+1)} - \lambda_{min}^{(k)}\right|}{\lambda_{min}^{(k+1)}} \le \varepsilon$$

where $\varepsilon = 10^{-2S}$, S - is a demanded number of significant figures that calculates the value (usually S=3).

The second algorithm of the critical load determination is based on the linear subspace iteration method (LSIM) [12]. According to the algorithm of this method at the end of each iterative cycle we form the matrix projections are stated:

$$[K]_{(k)} = [u]_{(k)}^T [K][u]_{(k)}$$

$$[K_г]_{(k)} = [u]_{(k)}^T [K_г][u]_{(k)}$$

$$[u]_{(k)} = [\{u\}_1 \{u\}_2 \ldots \{u\}_q]$$

where $_{(n\times q)}$ - is a matrix of iterated vectors which number of lines is equal to the order of matrixes $[K]$ and $[K_г]$, and the number of columns $q << n$ corresponds to the number of simultaneous iterated vectors. The problem of eigenvalues is solved by the Jacobi algorithm:

$$[K]_{(k)}\{X\}_{(k)} = [K_г]\{X\}_{(k)} \lambda_{min}^{(k)}$$

The norms of mistakes are used as a criterion of the iterative cycle termination:

$$\frac{\left\| [K]\{X\}_{(k)} - \lambda_{min}^{(k)}[K_г]\{X\}_{(k)} \right\|}{\left\| [K]\{X\}_{(k)} \right\|}$$

The nodal critical load vector is determined by the formula:

$$\{P_{кр}\} = \lambda_{min}\{P\}.$$

It is common knowledge that linear analysis of trussed structure stability gives the overestimated value of the critical load. It is connected with the computational scheme idealization (the lack of initial camber of truss members and the central application of forces), and also with the fact that in the global stiffness matrix the block of axial deformation is independent of the block of bending deformation. Real truss elements have initial geometrical imperfections which cause interrelation between axial and bending reactions.

At the same time the considered numerical method allows to give upper estimate of the critical load which value can be specified by using the FEM stepwise procedure.

ITERATIVE STABILITY ANALYSIS BY USING THE STEP PROCEDURE OF THE FINITE-ELEMENT METHOD

Elements of the geometrical stiffness matrix $[K_г]$ are nonlinear functions of compression stress. Therefore, the FEM computation process has to be organized according to the schedule of the step load increment when simultaneous updating of the matrix elements and control load-bearing capacity of the structure by the determined displacement values w at the end of each load step [12].

We think that the load increment P_i at the i - step occurs in quasi-static manner and by a small amount. The solution of a geometrically nonlinear task at each step will be made by the Newton's iteration method that consistently calculates of additional displacement in element nodes, caused by fastening to forces. Figure-1, a) graphically presents such an approach (for the three load steps) where the computational solution is shown as the step saw-toothed line.

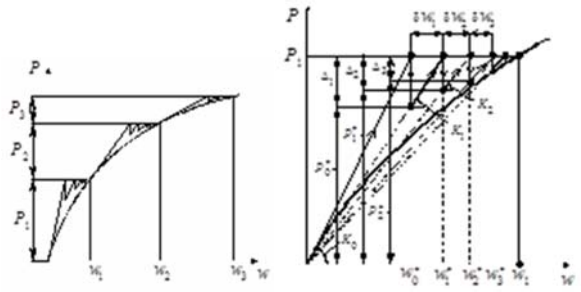

a) b)

Figure-1. Graphic imaging of the FEM computation process organized according to the schedule of the step load increment.

The FEM iterative algorithm on the example of the first load step (Figure-1, b) will be considered now. To simplify it Figure-1 omits curved and square brackets in vector and matrix notations.

The computational process is organized as follows:

a) The initial vector of nodal displacement by using the balance equation without regard to the geometrical stiffness matrix is calculated as follows:

$$\{w_0^*\}=[K]^{-1}\{P_1\},$$

where $[K]$ - is the total stiffness matrix;
$\{P_1\}$ - is a vector of nodal forces at the first load step.

b) The beginning of an iterative cycle $i=1, 2, \ldots, n_{max}$ (i - is the iteration index, n_{max} - is the maximum iteration indexes set by a computing engineer). By the determined values $\{w_{i-1}^*\}$ axis nodal reactions in *compression* finite elements are calculated and the geometrical stiffness matrix $[K_r(\{w_{i-1}^*\})]$ is formed. In notation $[K_r(\{w_{i-1}^*\})]$ the value in round brackets specifies that elements of the geometrical stiffness matrix depend on nodal displacement.

c) The sectional stiffness matrix $[K_i]$ relating to current iteration is formed:

$$[K_i]=[K]+[K_r(\{w_{i-1}^*\})].$$

d) Nodal reactions corresponding to the nodal displacement vector $\{w_{i-1}^*\}$ are calculated as follows:

$$\{P_{i-1}^*\}=[K_i]\{w_{i-1}^*\}.$$

e) The vector of fastening to nodal reactions is calculated as follows:

$$\{\Delta_i\}=\{P_1\}-\{P_{i-1}^*\}.$$

f) The additional nodal displacement vector $\{\delta w_i\}$ caused by the vector of fastening $\{\Delta_i\}$:

$$\{\delta w_i\}=[K_i]^{-1}\{\Delta_i\}.$$

g) The nodal displacement vector is corrected as follows:

$$\{w_i^*\}=\{w_{i-1}^*\}+\{\delta w_i\}.$$

h) Starting on the $i=2$, estimate of iterative procedure convergence with the following condition:

$$\|\delta w_i-\delta w_{i-1}\|<\varepsilon, \quad (2)$$

where $\|\delta w_i-\delta w_{i-1}\|=\sqrt{\{\delta w_i-\delta w_{i-1}\}^T\{\delta w_i-\delta w_{i-1}\}}$ - is an additional nodal displacement difference norm at complementary iterations;
$\varepsilon=10^{-8}$ - is a positive small quantity used for the end of the iterative process of refinement of solution.

The steps 2 - 8 repeat until the condition (2) is met or the number of iterations will not exceed n_{max}. Graphically the minimization of fastening to forces is a certain trajectory in the form of the saw-toothed line that is close to the desired point of solution (Figure-1, b).

The start of the second load step begins with the solution of a set of equations:

$$[[K]+[K_r(\{w_1\})]]\{w_0^*\}=\{P_2\},$$

where $\{w_1\}$ - is the nodal displacement vector formed on the first load step;
$\{P_2\}$ - is the vector of additional nodal forces corresponding to the second load step.

At the 3rd stage of the iterative process the *secant* stiffness matrix $[K_i]$ taking into account the data obtained at the first load step.

$$[K_i]=[K]+[K_r(\{w_1\}+\{w_{i-1}^*\})].$$

At the 7th stage 7 the nodal displacement vector correcting is conducted by the formula:

$$\{w_i^*\}=\{w_1\}+\{w_{i-1}^*\}+\{\delta w_i\}.$$

By analogy with the previous formula the calculations at the subsequent load steps by using the vectors $\{P_3\}, \{P_4\}, \ldots$ are carried out.

At each iteration in the course of the stepwise load process behavior of the vector $\{\delta w_i\}$ is controlled. Usually while nonlinear stability analyzing the value decrease $\{\delta w_i\}$ between complementary iterations testifies to the achievement of the stabilized condition by the system (process meets). The fact of loss of stability is the state when sizes increase from iteration to iteration (the process goes separate ways).

It should be noted that many elastic systems having achieved the bifurcation point can enter into a new steady state with the further load growth.

In passing to the next load step the studied structure configuration is automatically carried out.

MODELING AND ESTIMATE OF THE STRAIN-STRESS STATE OF A BUS BODY PILLAR WITH ACCOUNT FOR GEOMETRICAL NONLINEARITY

To determine the most dangerous section of bus body pillars and to study their strain-stress state under the influence of emergency load a mathematical model in the form of the thin-walled rectilinear rack of box-shaped section working for a bend will be developed [13]. Stress-strain behavior of the pillar material (steel): the elasticity modulus $E=2.05\cdot10^5$ mPa; the Poisson ratio ν =0.28; the yield stress σ_T =283 mPa. Figure-2 presents the configuration and the analytical model of a half of a pillar that is rigidly fixed by one end and loaded with the uniform load p on a site 40 mm in diameter. The gage is t = 2 mm. Numerical experiment has taken p_{max} = 8 mPa. On the parting site boundary conditions u_x =0; φ_y =0 were used (there are no displacement along the axis x

and the rotational angle about the axis y). Figure-3 presents the schedule of division of a half of a pillar into finite elements. Pillar site sampling is executed by plate finite SHELL43 [11] elements. In grid generating the options *smart* and *tri* were used. On a loaded site the thickness of elements is synthetically increased to 10 mm.

The numerical solution taking into account geometrical nonlinearity is obtained by the Newton's iteration method together with the stepwise load algorithm (N=50 steps).

Figure-4 presents the results of finite-element modeling in the form of the schedule *displacement~ load* ($p \sim u_z$) [14]. Displacement u_z was calculated in the site center of the application of load. The dashed line 1 corresponds to the linear solution; the line 2 describes a pillar bending with account for large displacements.

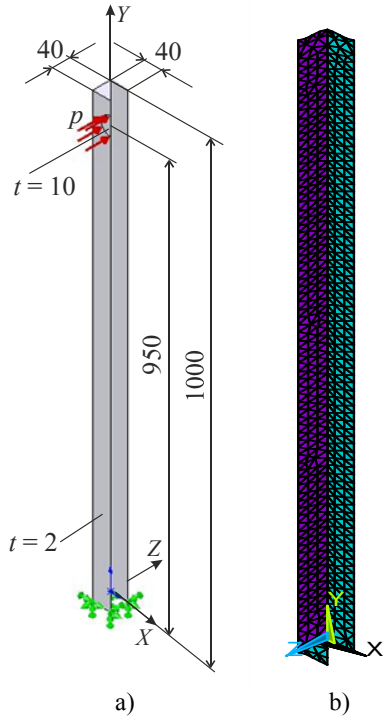

Figure-2. Configuration: a) and the analytical model; b) of a half of a pillar that is rigidly fixed by one end and loaded with the uniform load p on a site 40 mm in diameter.

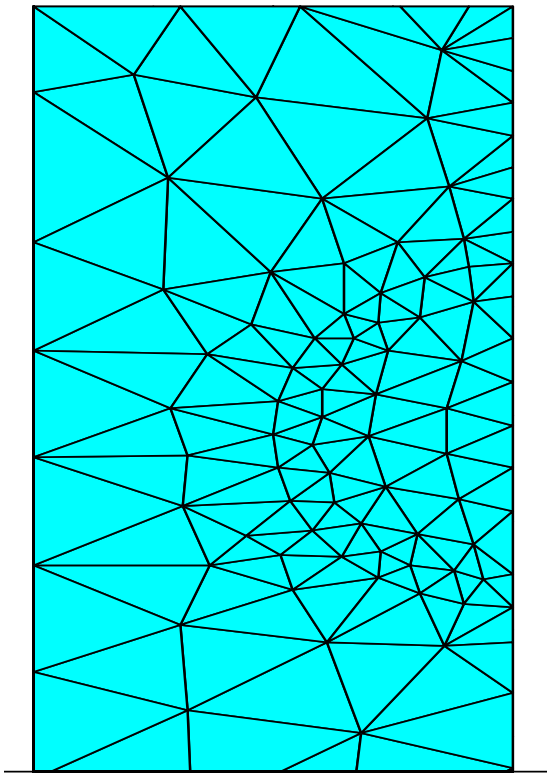

Figure-3. The schedule of division of a half of a pillar into finite elements.

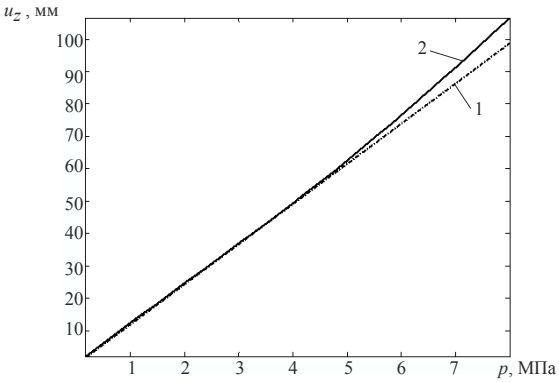

1 - a pillar bending in linear solving; 2 - a pillar bending with account for geometrical nonlinearity

Figure-4. Results of finite-element modeling in the form of the schedule displacement~ load ($p \sim u_z$).

Figures 5 and 6 present the pictures of the pillar deformation for load steps 10, 20, 30, 40 kN. Figure 6 shows the pillar sites which take with bedding-in for load steps 30 and 40 kN in detail.

As Figures 5 and 6 show that with increased load there is the local stability loss on the compressed pillar part that is shown in buckling of the corresponding surface

distortion. In the graph $p \sim u_z$ (Figure-4) in this place the line 2 runs the originally rectilinear direction out [15]. The calculations have showed the further load growth provides the monotonous beam deflection increase. Thus, the line 2 runs the line 1 more and more out. The warping effect amplifies that is shown in the growth of local deformations on the compressed pillar surface.

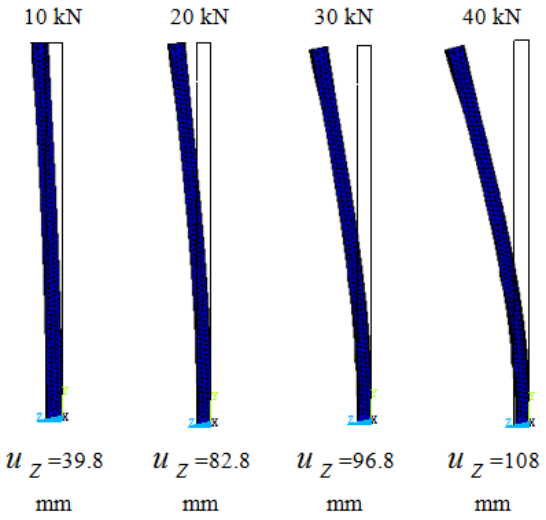

Figure-5. Pictures of pillar deformation for load steps 10, 20, 30, 40 kN.

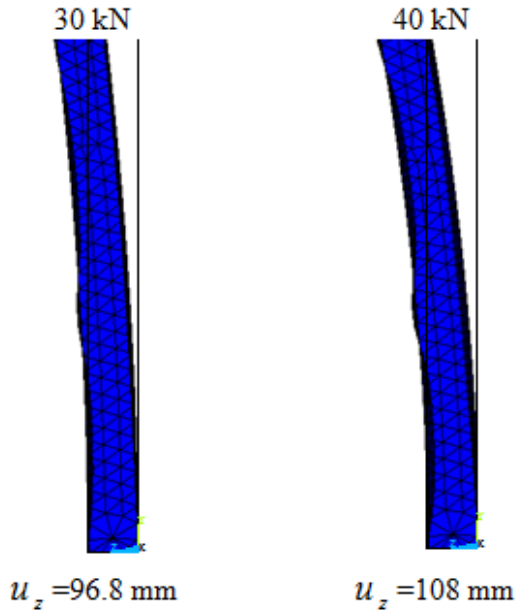

Figure-6. Enlarged pictures of the pillar deformation for load steps 30 and 40 kN.

Analysis of the obtained results allows us to draw a conclusion on adequate modeling of a bend of a the thin-walled pillar bending taking into account large displacements, namely, when in the course of the structure deformation there is a change of its analytical model. At the same time this type of numerical analysis leaves open the question of the influence of the material plastic response to the process of internal effort redistribution at large displacements.

REFERENCES

[1] GOST P 41.66-00 (UNECE Regulations No. 66). 2000. Uniform instructions concerning the approval of large-size passenger vehicles in a durability relationship of the upper structure. Brought on 26 May 1999, No. 184. Moscow: PPC Publishing House of standards. pp. 19.

[2] Kalmikov B.Y., Ovchnnikov N.A., Kalmikova O.M., Guguyev I.K. and Kushnariva I.V. 2015. Application of the method of distribution of the total energy of impact on the bearing elements of the body of the bus when calculating the failure loads. ARPN Journal of Engineering and Applied Sciences. 10(10): 4366-4371.

[3] Kalmikov B.Y., Visotski I.Y., Ovchinnikov N.A., Petriashvili I.M. and Kalmikova Y.B. 2015. The use of additional devices for reducing the deformation of the bus body when tipping. ARPN Journal of Engineering and Applied Sciences. 10(12): 5150-5156.

[4] Ovchinnikov N.A., Kalmikov B.Y., Stradanchenko S.G., Kozyreva E.A. and Chefranova O.V. 2015. The engineering method of calculation of the remaining life of the bus body safe operation on the basis of estimation of its corrosion deterioration. ARPN Journal of Engineering and Applied Sciences. 10(22): 10511-10522.

[5] Kalmikov B.Y., Ovchinnikov N.A., Kalmikova O.M., Jigulskii V.I. and Yurshin Y.G. 2015. Proposals for determining the impact energy at bus rollover for conditions of UNECE no.66. ARPN Journal of Engineering and Applied Sciences. 10(8): 3793-3797.

[6] Gepner B., Bojanowski C., Kwasniewski L. and Wekezer J. 2014. Effectiveness of ECE R66 and FMVSS 220 standards in rollover crashworthiness assessment of paratransit buses. International Journal of Automotive Technology. 15(4): 581-591.

[7] Li Z., Xiao Y., Zhu W. and Zhao H. 2013. The safety of body structure and occupant protection research of medium bus under three kinds of frontal impact

forms. Volume 197 Lecture Notes in Electrical Engineering. 9: 279-292. Code 99825.

[8] Jeyakumar P.D. and Devaradjane G. 2012. Improvement of the frontal structure of a bus for crash accidents. ASME International Mechanical Engineering Congress and Exposition, Proceedings (IMECE). 11: 183-187.Code 100737.

[9] Wang R., Zhang X.-Y., Feng H. and Chen J.-G. 2014. Simulation and improvement of bus rollover against barrier. Zhendong yu Chongji. Journal of Vibration and Shock. 33(6): 40-43.

[10] Karliński J., Ptak M., Dzialak P. and Rusiński E. Strength analysis of bus superstructure according to Regulation No. 66 of UN/ECE. Archives of Civil and Mechanical Engineering. 14(3): 342-353.

[11] Basov K.A. 2005. ANSYS: User's reference book. Moscow: DMK Press. p. 640.

[12] Belkin A.E. 2008. Plating design by using the finite-element method: Work book. Moscow: BMSTU Publishing House. p. 232.

[13] Ovchinnikov N. A. 2013. Finite-element analysis of the strain-stress state of elements of cross lateral power bus body sections in use. Don Engineering Bulletin. 25(2), (25): 9.

[14] Kalmykov B.Yu. and Ovchinnikov N.A. 2010. Technical in-use bus condition estimate maintenance. Motor transportation enterprise. 2: 19-23.

[15] Kalmykov B.Yu., Vysotsky I.Yu., Ovchinnikov N. A. and Bocarov S.V. 2012. The way to determine the bus dumps height for estimate of its body structural strength by the UNECE Regulations No. 66. Don Engineering Bulletin. 21(3): 10-17.